ResearchGate

See discussions, stats, and author profiles for this publication at: https://www.researchgate.net/publication/257952926

Germanium metal–semiconductor–metal photodetectors evanescently coupled with upper-level silicon oxynitride dielectric waveguides

Article *in* Applied Physics Letters · December 2012

DOI: 10.1063/1.4773212

CITATIONS
5

READS
35

7 authors, including:

Alfonso Torres Jacome
Instituto Nacional de Astrofísica, Óptica y Electrónica (INAOE)

197 PUBLICATIONS **729** CITATIONS

SEE PROFILE

Joe C Campbell
University of Virginia

735 PUBLICATIONS **13,875** CITATIONS

SEE PROFILE

Ignacio Enrique Zaldivar Huerta
Instituto Nacional de Astrofísica, Óptica y Electrónica (INAOE)

23 PUBLICATIONS **40** CITATIONS

SEE PROFILE

Some of the authors of this publication are also working on these related projects:

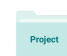

Optical design with optical components fabricated on silicon substrates View project

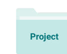

Low Temperature Detectors Development @ INAOE View project

All content following this page was uploaded by Ignacio Enrique Zaldivar Huerta on 17 March 2016.

The user has requested enhancement of the downloaded file.

Germanium metal-semiconductor-metal photodetectors evanescently coupled with upper-level silicon oxynitride dielectric waveguides

Juan C. Cervantes-González,[1,a)] Donghwan Ahn,[1,b)] Xiaoguang Zheng,[2]
Sanjay K. Banerjee,[1] Alfonso T. Jacome,[3] Joe C. Campbell,[2]
and Ignacio E. Zaldivar-Huerta[3]
[1]*Microelectronics Research Center, The University of Texas at Austin, Austin, Texas 78712, USA*
[2]*Department of Electrical and Computer Engineering, University of Virginia, Charlottesville, Virginia 22904, USA*
[3]*Instituto Nacional de Astrofísica, Óptica y Eletrónica (INAOE), Puebla, Pue. 72000, Mexico*

(Received 11 September 2012; accepted 10 December 2012; published online 28 December 2012)

We demonstrate Ge-on-Si metal-semiconductor-metal (MSM) photodetectors monolithically integrated with silicon oxynitride (SiO_xN_y) waveguides. The waveguide is placed on top of the photodetector and between the metal electrodes, evading the shading effect by metal electrodes, which is typical in surface-illuminated MSM photodetectors. The devices showed responsivity of about 0.45 A/W for 80 μm long devices at 1550 nm. The photodetector with 1.5 μm electrode spacing showed 3 dB bandwidth of 2.0 GHz at −2 V and 2 μA dark current. Further studies suggest that with a modified design the structure is capable of achieving 1 A/W responsivity and greater bandwidth. © *2012 American Institute of Physics*. [http://dx.doi.org/10.1063/1.4773212]

Monolithic integration of photonic components with current microelectronics technology is a possible solution to the terabit-per-second future data transfer demand for chip-to-chip and intra-chip interconnections. In recent years, such a monolithic integration approach based on Si complementary metal–oxide–semiconductor (CMOS)-compatible processes has shown promising potential.[1,2] One of the key photonic devices in optical interconnects is the waveguide (WG)-integrated photodetector needed at the end of the optical link.

Many waveguide-integrated Ge-on-Si photodetectors have demonstrated high performances compared to surface-illuminated photodetectors, including p-i-n[3–5] and metal-semiconductor-metal (MSM)[6–8] detector structures, with different coupling structures such as bottom-waveguide-coupled,[3–7] and butt-waveguide-coupled[8] devices. Many of those were integrated with Si waveguides built on silicon-on-insulator (SOI) wafers. However, because Si waveguides built in SOI wafers share the same Si layer with CMOS devices, Si waveguide networks occupy the CMOS chip real estate and can interfere with microelectronics design layout.

On the other hand, dielectric waveguides such as SiN_x or SiO_xN_y can be introduced in the upper level in the chip. With optical waveguides built in the upper level instead of on the substrate, the general Si CMOS chip architecture, where active devices are fabricated on the substrate and the passive interconnects are in the upper levels, can be retained for easier electronic-photonic integration. A top-WG-coupled photodetector can fit better with such optical interconnect architecture. Ge p-i-n[9] and Si p-i-n[10] PD devices with the top-WG-coupling scheme have been demonstrated.

In this paper, we present a crystalline Ge MSM photodetector integrated with SiO_xN_y channel waveguides using a top-WG-coupled configuration. MSM photodetectors often provide simple device structure and processing, faster speed response, and better compatible integration with CMOS transistors. The main disadvantage of a surface-illuminated MSM-PD is often its low responsivity due to the shading effect by the metal electrodes and relatively small photodetector film thickness. However, such problem can be overcome by achieving a proper integration with a waveguide between the MSM metal electrodes, which is the motivation of this work. Also, SiN_x or SiO_xN_y waveguides can be integrated in the back end of line (BEOL) of CMOS processes, which would be advantageous for applications in three-dimensional (3D) integrated photonic circuits.

The integrated photodetector design consists of a SiO_xN_y channel waveguide laid on top of a Ge MSM device and between the MSM metal electrodes, as shown in Fig. 1(a). The fabrication process started with (100) Si p$^-$ (10–20 Ω cm) substrates. The wafers were cleaned with standard piranha

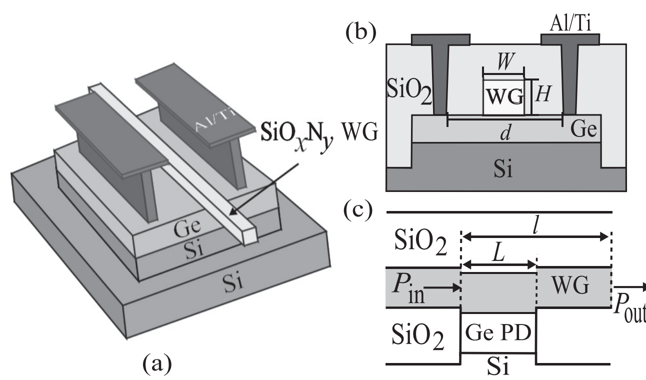

FIG. 1. (a) 3D-schematic structure and (b) cross-section of the top-WG-coupled PD device. (c) Schematic of the waveguide photodetector coupling structure with some notations used in Eq. (1).

a)Present address: Intel Labs, Tlaquepaque, Jal. 45600, Mexico.
b)Author to whom correspondence should be addressed. Electronic mail: donghwan.ahn@gmail.com. Present address: Samsung Electronics U.S. R&D Center (SAIT-USA), Cambridge, Massachusetts 02142, USA.

 © 2012 American Institute of Physics

Downloaded 02 Jan 2013 to 187.135.36.24. Redistribution subject to AIP license or copyright; see http://apl.aip.org/about/rights_and_permissions

solution and HF dip. Epitaxial growth of Ge was then performed in an ultrahigh vacuum chemical vapor deposition (UHVCVD) system at a pressure of 10^{-9} Torr. An ultrathin Si seed (∼15 nm) was grown at 700 °C. Subsequently, a thin relaxed Ge layer (∼50 nm) was grown at 380 °C to minimize the dislocation density, and followed by an additional Ge main layer growth of 1.25 μm at 700 °C. The devices were fabricated using mesa structures where 2.5 μm of Ge/Si was etched to reduce the optical losses of the waveguide into the Si substrate. Then, the SiO_2 cladding layer was deposited by plasma-enhanced chemical vapor deposition (PECVD), and the top surface was planarized with chemical-mechanical polishing (CMP). Next, SiO_2 windows were opened on top of the Ge layer to assure a good optical contact between the waveguide and photodetector material. Then, a layer of 1.2 μm thick SiO_xN_y was deposited by PECVD, and the waveguide structure was patterned using the contact lithography. SiO_xN_y material has the advantage of providing a wide and flexible range of refractive index, which can be adjusted by oxygen and nitrogen composition changes.[11] The single mode channel waveguide design we used had 1 μm(W) × 1.2 μm(H) dimensions, and a refractive index of 1.64. After waveguide etching, a 2.5 μm thick SiO_2 cladding layer was deposited by PECVD. Finally, contact holes were opened and 25 nm Ti and 1.2 μm aluminum were deposited by evaporation. After the lift-off of the contact pads, the wafers were annealed at 400 °C for 20 min in forming gas. The fabricated photodetectors have a device length, L, of 10, 40, and 80 μm, a width of 10 μm, and an electrode spacing, d, of 1.5, 2.0, and 3 μm.

Photodetectors were characterized by taking measurements of DC responsivity, dark current-voltage characteristics, and frequency response. The responsivity of the waveguide-integrated photodetector, with 1550 nm illumination coupled to the detector through the waveguide, was measured by coupling the light using a microlensed fiber into the cleaved facet of the SiO_xN_y waveguide at the edge of the chip. The optical power at the point of entering the photodetector, P_{in} (see Fig. 1(c)), was estimated using the method similarly reported in Ref. 9. The responsivity is given by

$$R = \frac{\Delta I}{P_{in}} = \frac{I - I_{dark}}{P_{out,ref} \times 10^{\alpha_{WG} \cdot l/10}}, \quad (1)$$

where ΔI is the change of the current under illumination, α_{WG} is the waveguide transmission loss in units of dB/cm, l is the distance from the photodetector input to the end of the waveguide, and $P_{out,ref}$ is the transmitted optical power of the reference waveguide. Being measured from adjacent reference waveguides using the cutback method, the waveguide propagation loss at 1550 nm was estimated to be 8.2 dB/cm, which can be improved further when the fabrication processing details are optimally developed with advanced processing facilities.[11] The waveguide propagation loss was not much optimized in our work, because it is not the focus of this paper. Defining P_{in} in Eq. (1) as the optical power that was delivered to the front of the photodetector and entering the device enable us to exclude the factor of the passive waveguide loss and to evaluate the photodetector performance mostly based on (1) the optical coupling efficiency from the passive bus waveguide to the photodetector and (2) the photodetector conversion efficiency.

Figure 2 shows the measured responsivity of the SiO_xN_y waveguide-integrated Ge MSM photodetectors. The 0.45 A/W responsivity for an 80 μm long device shown in Fig. 2 indicates the external quantum efficiency of ∼36%, which includes both WG-to-PD optical coupling and internal PD quantum efficiency. Limited responsivity of our device seems to be due to optical leakage of unabsorbed light into the Si substrate attributed to weak optical confinement in the Ge/Si interface and a relatively small proportion of the horizontal WG-to-PD direct coupling due to small index-contrast of the waveguide,[10,12] which will be further explained in the next paragraph. Comparison to the surface-illuminated device in Fig. 2 shows that a waveguide-integrated photodetector device can achieve significantly higher responsivity compared to the similar Ge MSM PDs that are surface-normal illuminated. Surface-illuminated MSM photodetectors lose efficiency due to metal electrode shading and limited Ge film thickness. Integration with waveguides can evade the shading effect by injecting the light only in the middle of the electrodes spacing, and achieve the lateral light coupling to the photodetector, thus resulting in higher effciency.

The dark-current characteristics of our devices are shown in the Fig. 2 inset which showed reasonably low 1-2 μA dark current level in the bias voltage range of 1–3 V. The dark current for longer devices gradually increased up to 8 μA for 80 μm long devices at 3 V, relatively higher compared to that observed for the Ge PIN device which can be <1 μA with approximately similar device sizes.[9] High dark currents in the MSM devices may be because of the low Schottky barrier height for any metal on Ge, and can be further lowered by adding some known processing measures such as amorphous Ge[13] or a silicon-carbon (Si:C)[7] Schottky barrier enhancement layer.

Fig. 3 shows the responsivity change in terms of the photodetector coupling length. The responsivity increases at a rate of $1/\alpha_{coupling} \sim 33$ μm, and tends to saturate at about >60 μm. The WG-to-PD coupling rate of our photodetector tends to be longer compared to that of Ge devices coupling

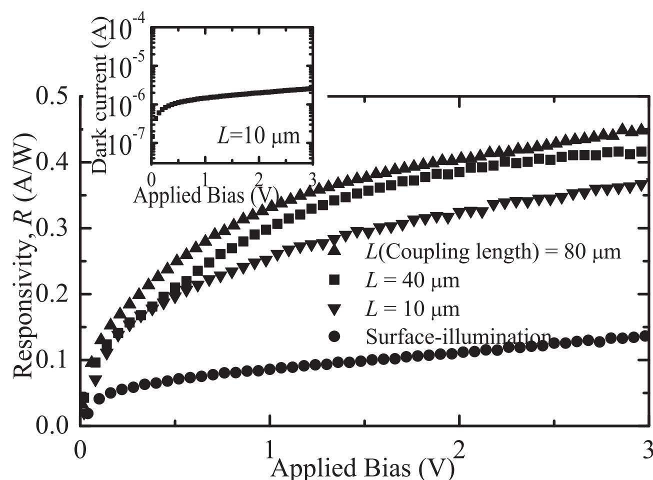

FIG. 2. Responsivity as a function of voltage measured for a detector length of 10, 40, and 80 μm. The circle line indicates the responsivity of the device when illuminated by optical fiber from the top. The inset shows the dark current-voltage curve for $L = 10$ μm.

Downloaded 02 Jan 2013 to 187.135.36.24. Redistribution subject to AIP license or copyright; see http://apl.aip.org/about/rights_and_permissions

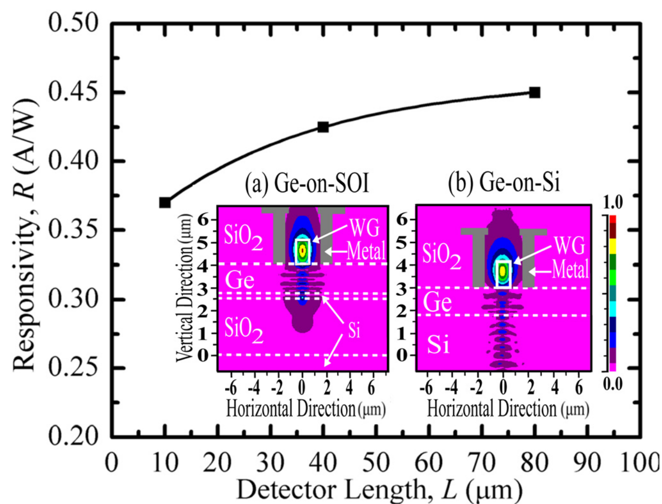

FIG. 3. Measured and fitted data of responsivity vs device length. The inset shows the optical simulation (cross-section view) of the mode profile with (a) Ge-on-SOI and (b) Ge-on-Si substrates. The use of SOI substrates allows the confinement of the light between the waveguide and the buried oxide.

case with Si waveguides.[5,7] However, a higher responsivity and a shorter coupling length can be achieved with further modifications in the device structure design. For example, use of a higher index-contrast Δn waveguide can enable a greater portion of light from the WG to enter the Ge layer in the horizontal direction, decreasing the detector coupling length. Also, the use of SOI substrate instead of Si bulk wafer can confine the photons in the Ge layer until they are fully absorbed in the photodetector (Fig. 3 inset (a)), whereas the photons left unabsorbed after a single pass through thin Ge film leaks into Si, and can get lost in the case of the device built on Si bulk substrate (Fig. 3 inset (b)). Therefore, the responsivity performance of our Ge MSM devices can be enhanced further simply by adopting SOI substrates for the same device structure.

In Fig. 4, the frequency response is plotted for the device with a 2 μm electrode spacing at 2 V bias voltage. In the Fig. 4 inset, the measured 3 dB frequency results of the devices with different electrode spacings are shown. As it is

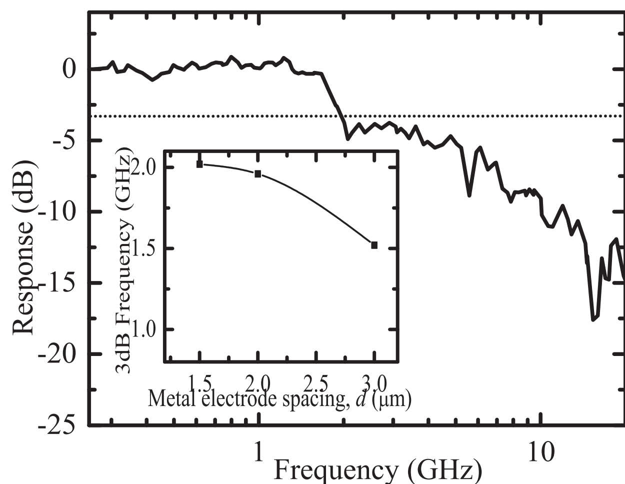

FIG. 4. Frequency response for the device with a $d = 2\,\mu$m. The inset shows 3 dB frequency measured at 1.55 μm wavelength and 2 V for different electrode spacings.

shown, with decreasing the electrode spacing, the 3 dB frequency increases, reaching approximately 2.0 GHz at 2 V. In MSM-PDs, the bandwidth is related to the Ge thickness, and the spacing of electrodes. The increase of the frequency response speed tends to be saturating at <1.5 μm electrode spacing, because the photon absorption that occurs in the lower part of Ge film deep below the surface, where the electric field intensity would be weak, remains to be significant portion in spite of the decreased electrodes spacing and becomes a limiting factor. In our structure, a higher bandwidth can be achieved by decreasing the waveguide dimensions and using SOI substrates. Smaller waveguide dimensions and SOI substrates allow for the decrease of the spacing electrode and the Ge thickness, respectively, and can shorten the transit time of the collected carrier while maintaining a high responsivity.

We demonstrated CMOS-compatible MSM Ge-on-Si photodetectors monolithically integrated with SiO_xN_y waveguides using top-WG-coupling configuration. The dark current is about 2 μA for a 10 μm long photodetector, which can be reduced by increasing the Schottky barrier height. The responsivity is about 0.45 A/W for an 80 μm long photodetector, and the 3 dB frequency reaches about 2.0 GHz for a 1.5 μm wide electrode spacing. We experimentally demonstrated that, for the same-quality Ge MSM photodetector devices, optical signal injection through a waveguide in the middle of the spacing between the metal electrode can provide significantly higher efficiency and speed, compared to the surface-normal illuminated case of the same photodetectors. Our device can fit well for the architecture that employs a dielectric waveguide network in the upper level, and we discussed the design methods to further enhance the device performance using high index-contrast waveguides, smaller waveguide dimensions, and SOI substrates.

[1]R. Soref, IEEE J. Sel. Top. Quantum Electron. **12**, 1678 (2006).
[2]L. C. Kimerling, D. Ahn, A. B. Apsel, M. Beals, D. Carothers, Y.-K. Chen, T. Conway, D. M. Gill, M. Grove, C.-Y. Hong, M. Lipson, J. Liu, J. Michel, D. Pan, S. S. Patel, A. T. Pomerene, M. Rasras, D. K. Sparacin, K.-Y. Tu, A. E. White, and C. W. Wong, Proc. SPIE **6125**, 612502 (2006).
[3]S. Liao, N.-N. Feng, D. Feng, P. Dong, R. Shafiiha, C.-C. Kung, H. Liang, W. Qian, Y. Liu, J. Fong, J. E. Cunningham, Y. Luo, and M. Asghari, Opt. Express **19**, 10967 (2011).
[4]N.-N. Feng, P. Dong, D. Zheng, S. Liao, H. Liang, R. Shafiiha, D. Feng, G. Li, J. E. Cunningham, A. V. Krishnamoorthy, and M. Asghari, Opt. Express **18**, 96 (2010).
[5]J. Wang, W. Y. Loh, K. T. Chua, H. Zang, Y. Z. Xiong, T. H. Loh, M. B. Yu, S. J. Lee, G.-Q. Lo, and D.-L. Kwong, IEEE Electron Device Lett. **29**, 445 (2008).
[6]S. Assefa, F. Xia, S. W. Bedell, Y. Zhang, T. Topuria, P. M. Rice, and Y. A. Vlasov, Opt. Express **18**, 4986 (2010).
[7]K.-W. Ang, S. Zhu, M. Yu, G.-Q. Lo, and D.-L. Kwong, IEEE Photon. Technol. Lett. **20**, 754 (2008).
[8]L. Vivien, D. Marris-Morini, J.-M. Fédéli, M. Rouviére, J.-F. Damlencourt, L. E. Melhaoui, X. L. Roux, P. Crozat, J. Mangeney, E. Cassan, and S. Laval, Appl. Phys. Lett. **92**, 151114 (2008).
[9]D. Ahn, C.-Y. Hong, J. Liu, W. Giziewicz, M. Beals, L. C. Kimerling, J. Michel, J. Chen, and F. X. Kärtner, Opt. Express **15**, 3916 (2007).
[10]D. Ahn, C.-Y. Hong, L. C. Kimerling, and J. Michel, Appl. Phys. Lett. **94**, 081108 (2009).
[11]R. Germann, H. W. M. Salemink, R. Beyeler, G. L. Bona, F. Horst, I. Massarek, and B. J. Offrein, J. Electrochem. Soc. **147**(6), 2237–2241 (2000).
[12]D. Ahn, L. C. Kimerling, and J. Michel, J. Lightwave Technol. **28**, 3387 (2010).
[13]J. Oh, S. K. Banerjee, and J. C. Campbell, IEEE Photon. Technol. Lett. **16**, 581 (2004).

Downloaded 02 Jan 2013 to 187.135.36.24. Redistribution subject to AIP license or copyright; see http://apl.aip.org/about/rights_and_permissions
View publication stats